

Magnetically triggered release of molecular cargo from iron oxide nanoparticle loaded microcapsules

Susana Carregal-Romero^{1,2#}, Pablo Guardia^{3#}, Xiang Yu¹, Raimo Hartmann¹, Teresa Pellegrino^{3*}, Wolfgang J. Parak^{1,2*}

¹ Fachbereich Physik, Philipps Universität Marburg, Marburg, Germany

² CIC Biomagune, San Sebastian, Spain

³ Italian Institute of Technology, Genova, Italy

both authors contributed equally to this work

* corresponding authors: teresa.pellegrino@iit.it, wolfgang.parak@physik.uni-marburg.de

SUPPORTING INFORMATION

Contents

- I) Characterization of magnetic nanoparticles
- II) Characterization of polyelectrolyte capsules loaded with magnetic nanoparticles and Cascade Blue-labelled dextran
- III) TEM images of polyelectrolyte capsules before and after AMF treatment
- IV) Absorption spectra of the polyelectrolyte capsule components
- V) Confocal microscopy analysis of Cascade Blue-labelled dextran release
- VI) Hyperthermia experiments
- VII) References

I) Characterization of magnetic nanoparticles

Transmission electron microscopy (TEM) images of iron oxide nanoparticles (NPs) with hydrophobic capping, as yielded directly from the synthesis in organic solvents (Fig. S-I.1), and TEM images of the same NPs after a phase transfer to aqueous solution (Fig. S-I.2) are shown.¹ Fig. S-I.3 shows the hydrodynamic diameter and the zeta potential of the NPs in water obtained with dynamic light scattering (DLS) and Laser Doppler Velocimetry (LDV), respectively.

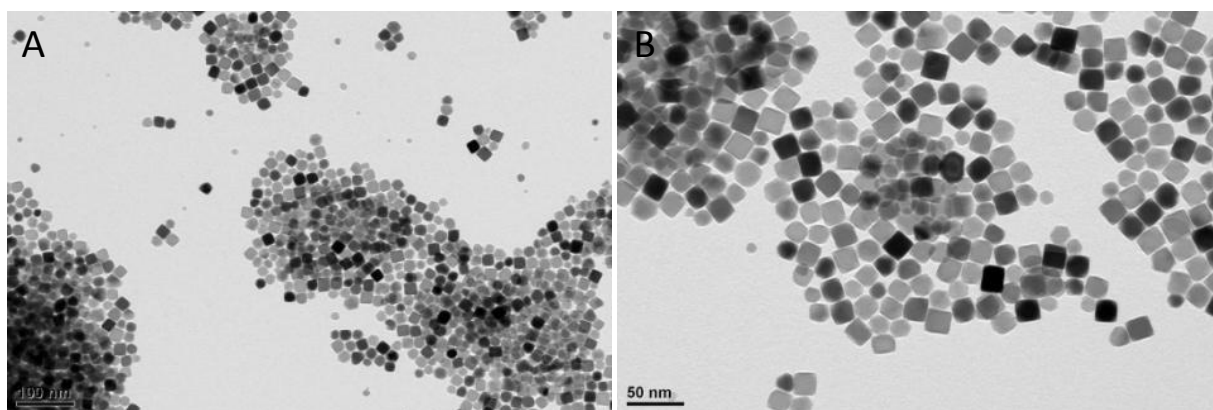


Fig. S-I.1 TEM images of hydrophobic iron oxide nanocubes in chloroform, after drying on a TEM grid. The scale bars correspond to 100 nm (A) and 50 nm (B).

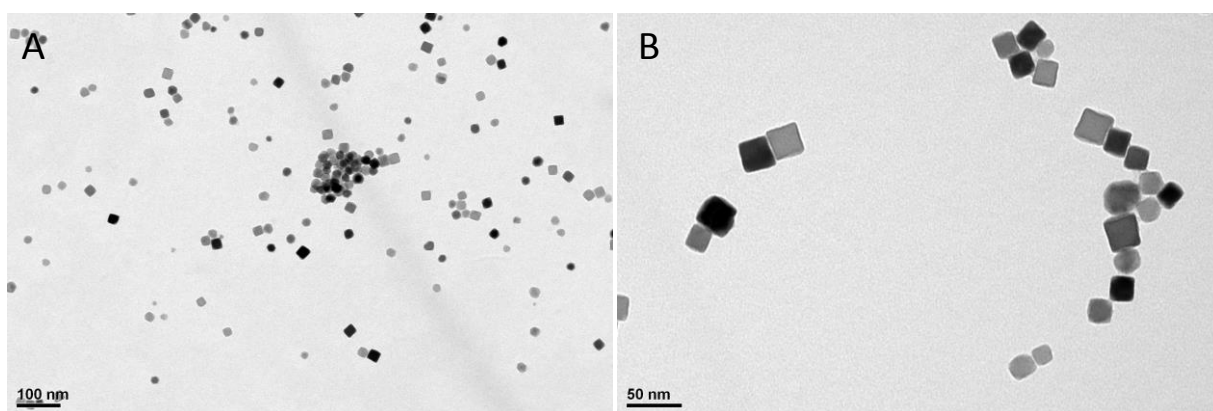


Fig. S-I.2 TEM images (A, B) of water-soluble iron oxide nanocubes used to produce the polyelectrolyte capsules. The scale bars correspond to 100 nm (A) and 50 nm (B).

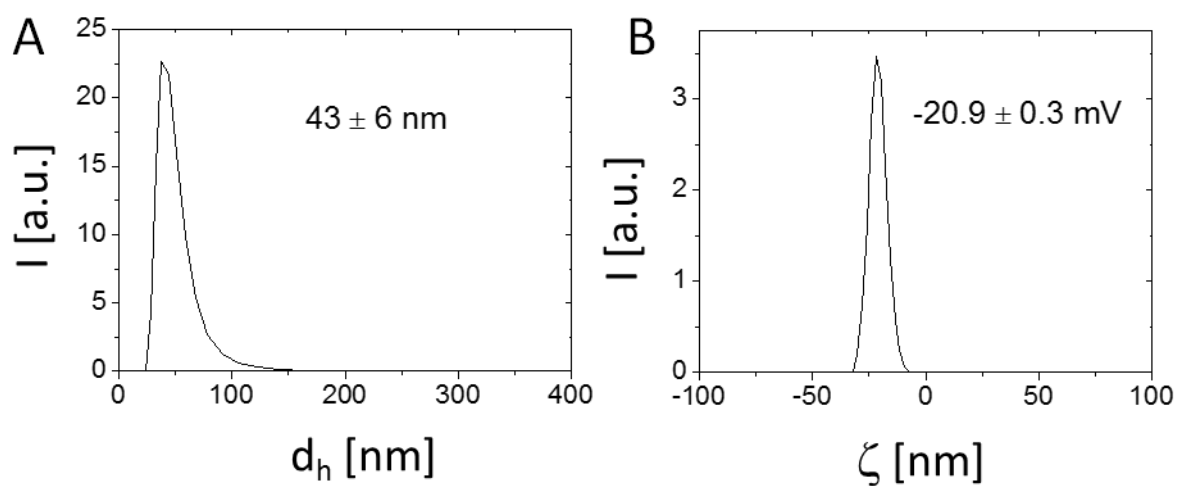


Fig. S-1.3 Distributions of the hydrodynamic diameter d_h (A) and ζ -potential (B) of the iron oxide NPs, as determined in Milli-Q water. The shown values are the result of three independent measurements.

II) Characterization of polyelectrolyte capsules loaded with magnetic nanoparticles and Cascade Blue-labelled dextran

TEM images of polyelectrolyte capsules decorated with iron oxide nanocubes in the shell at different magnifications (Fig. S-II.1).

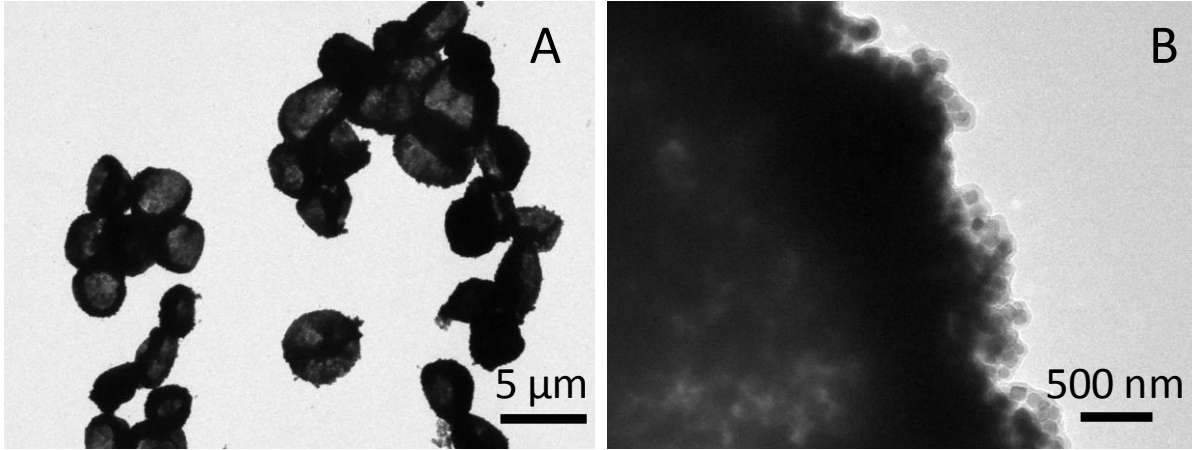


Fig. S-II.1 TEM images at different magnifications of polyelectrolyte capsules decorated with iron oxide nanocubes. The scale bars correspond to 5 μm (A) and 500 nm (B).

The concentration of capsules was obtained by counting with a hemocytometer. This was possible due to their micrometre size of the capsules. Induced Coupled Plasma-Atomic Emission Spectroscopy (ICP-AES) was used to obtain a concentration of 4.8 g/L of Fe in the polyelectrolyte capsule sample ($9.9 \cdot 10^8$ capsules/mL). In this way also the amount of iron per capsule could be determined to be 4.8 g/L / $9.9 \cdot 10^8$ capsules/mL = $4.8 \cdot 10^{-12}$ g Fe per capsule.

Having a side length of $d_c = 18$ nm the volume of each iron oxide nanocube is $V_{NP} = d_c^3 = 5832 \text{ nm}^3 \approx 5.8 \cdot 10^{-18} \text{ cm}^3 = 5.8 \cdot 10^{-24} \text{ m}^3$. The density of Fe_3O_4 NPs is approximately $\rho_{\text{Fe}_3\text{O}_4} \approx 5 \text{ g/cm}^3$. The mass of one iron oxide nanocube thus is $m_{NP} = V_{NP} \cdot \rho_{\text{Fe}_3\text{O}_4} = 2.9 \cdot 10^{-17} \text{ g}$. The ratio of iron/oxygen is 3/4, whereby each iron atom has 55.845 atomic mass units, and each oxygen 15.9994 atomic mass units. Thus, the percentage of mass of each iron oxide nanocube which is governed by iron is $(3 \cdot 55.845) / (3 \cdot 55.845 + 4 \cdot 15.9994) \approx 0.72$. Thus the mass of iron in each iron oxide NP is $m_{\text{Fe},NP} = 0.72 \cdot m_{NP} \approx 2.1 \cdot 10^{-17} \text{ g}$. In the above described case this means that the number $N_{NP/\text{capsule}}$ of iron oxide nanocubes per capsule is $4.8 \cdot 10^{-12} \text{ g Fe per capsule} / 2.1 \cdot 10^{-17} \text{ g Fe per NP} = 2.3 \cdot 10^5$ NPs per capsule.

Each capsule has diameter of $d = 4.6 \mu\text{m}$. With a shell composed out of 4 polyelectrolyte bilayers the shell thickness of the (PSS/PAH)(PSS/P(Am-DDA) NPs (PAH)(PSS/PAH)₂ capsules is $d_{\text{shell}} = 8 \cdot 1.5 \text{ nm} = 12 \text{ nm}$, assuming a thickness of 1.5 nm of each polymer layer. The volume of each capsule shell thus is $V_{\text{shell}} = 4\pi \cdot (d/2)^2 \cdot d_{\text{shell}} = \pi \cdot d^2 \cdot d_{\text{shell}} \approx 8.0 \cdot 10^{-19} \text{ m}^3$. The volume of all NPs in the shell of one capsule is $V_{NP \text{ in shell}} = N_{NP/\text{capsule}} \cdot V_{NP} \approx 1.3 \cdot 10^{-18} \text{ m}^3$. This results in $N_{NP/\text{capsule}} \cdot V_{NP} > V_{\text{shell}}$! The reason is that the thickness of the polymer shell $d_{\text{shell}} = 12 \text{ nm}$ is smaller than the side length $d_c = 18 \text{ nm}$ of one iron oxide nanocube. Thus one can say that the sample has an effective package fraction $N_{NP/\text{capsule}} \cdot V_{NP} / V_{\text{shell}}$ approaching 100%. This is also suggested by the TEM images, in which the shells are fully covered by NPs.

III) TEM images of polyelectrolyte capsules before and after AMF treatment

High (Fig. S-III.1) and low (Fig. S-III.2) resolution TEM images of polyelectrolyte capsules (with iron oxide nanocubes in the shell) before and after alternating magnetic field (AMF) treatment (300 kHz, 24 kAm^{-1}) for 90 minutes.

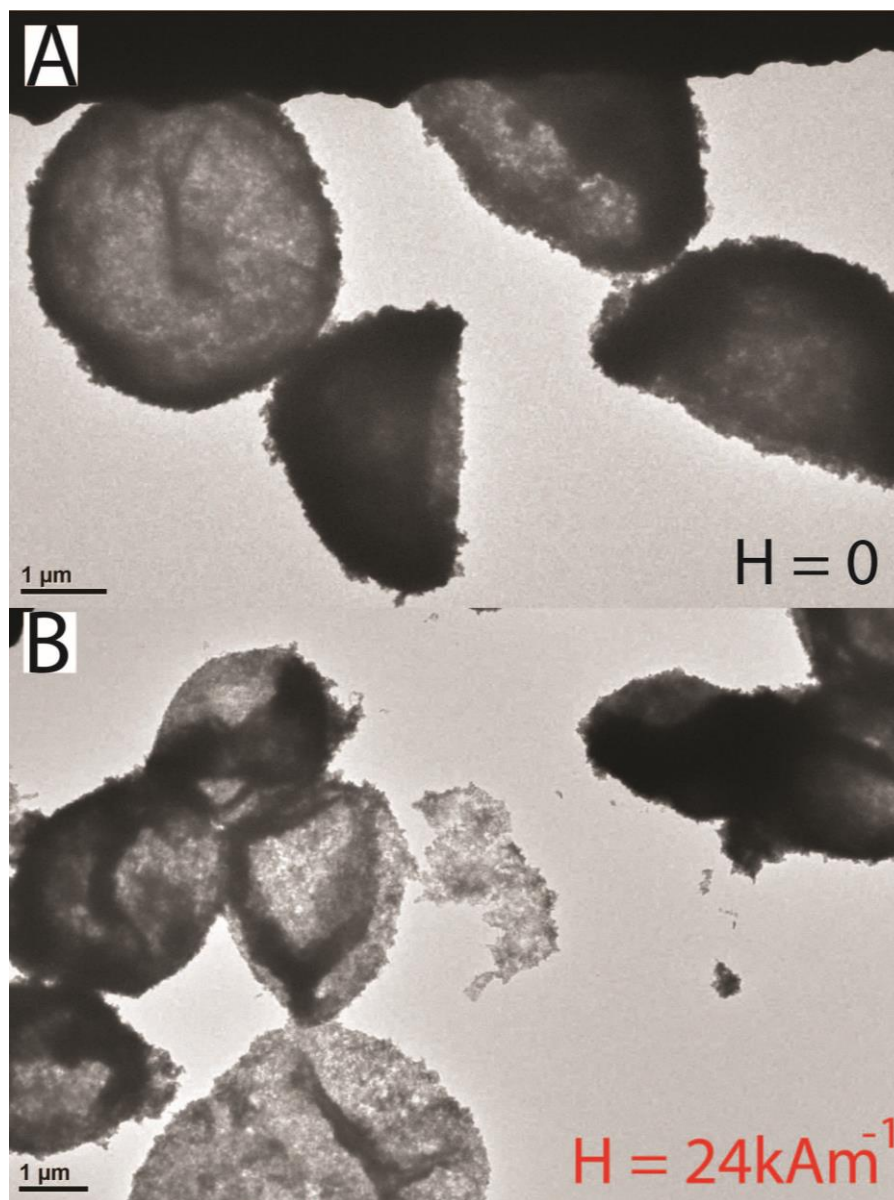


Fig. S-III.1 TEM images of polyelectrolyte microcapsules decorated with iron oxide NPs before (A) and after (B) being exposed to an AMF (300 kHz, 24 kAm^{-1}) for 90 minutes. Notice the detached NPs on panel B.

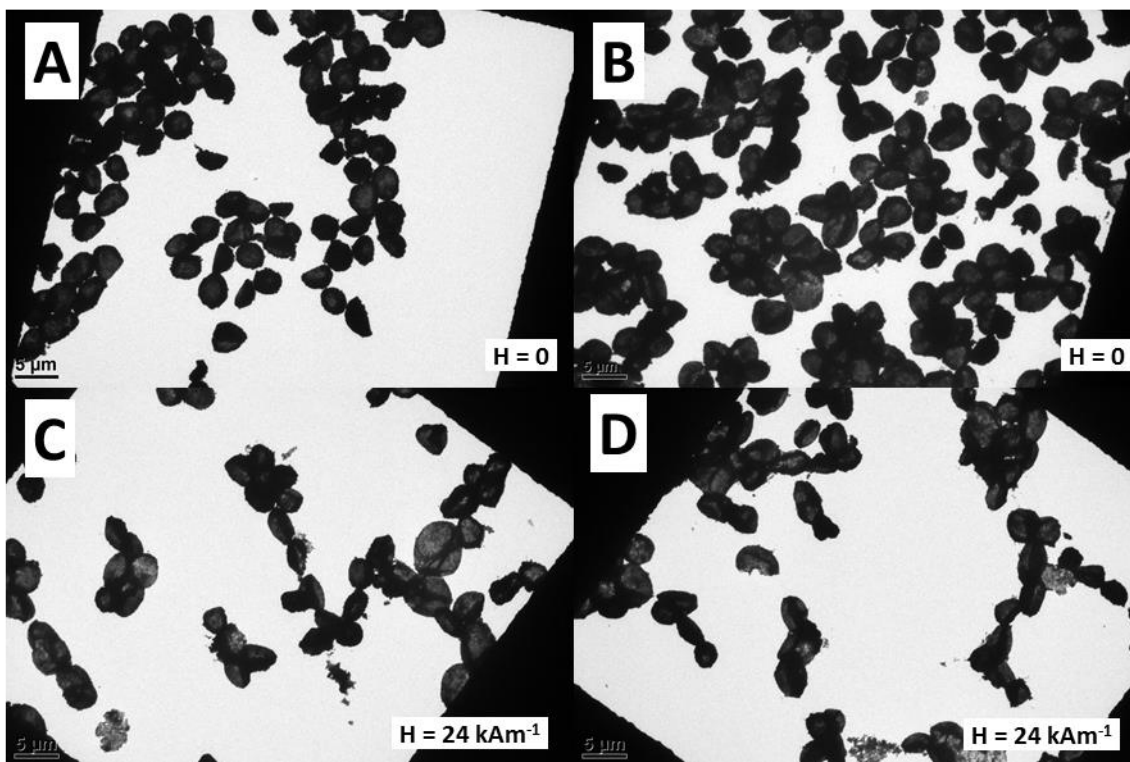


Fig. S-III.2 Low magnification TEM images of polyelectrolyte microcapsules decorated with iron oxide NPs before (A, B) and after (C,D) being exposed to an AMF (300 kHz, 24 kAm^{-1}) for 90 minutes. Notice the broken capsules as well as the detached NPs on panel C and D.

IV) Absorption spectra of the polyelectrolyte capsule components

UV-vis absorption spectra of all the components present in the polyelectrolyte capsules were measured in Milli-Q water and are reported in Fig. S-IV.1.

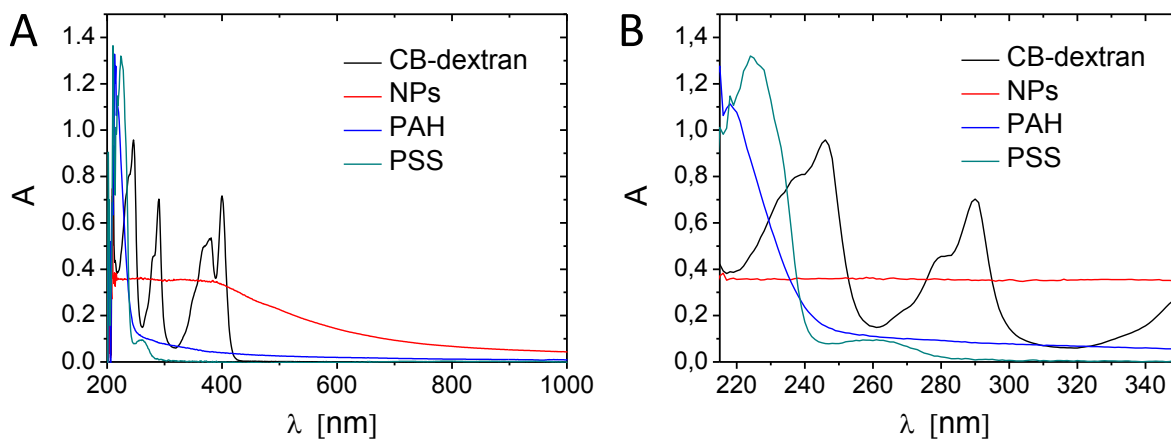


Fig. S-IV.1 Absorption spectra of the polyelectrolyte capsule components: Cascade Blue-labelled dextran (CB-dextran), magnetic NPs (NPs), poly (allylamine hydrochloride) (PAH), and poly (styrene sulfonate) (PSS). (A) Shows the obtained spectra ranging from 200 to 1000 nm and (B) is an enlargement showing only the absorption peaks between 215 and 350 nm.

V) Confocal microscopy analysis of Cascade Blue-labelled dextran release

The release of Cascade Blue-labelled dextran was studied also by confocal microscopy, which was used to compare the amount of Cascade Blue-dextran still encapsulated in the polyelectrolyte capsules after AMF irradiation. For this, the treated and non-treated capsules were separated from their corresponding supernatant and were further washed two times with Milli-Q water. Then confocal images were taken. The analyzing toolbox was programmed in MATLAB R2010a and it was programmed to recognize circular objects in the images. The toolbox calculated the size or the mean fluorescence intensity value inside these circles in one or more channels.

A sample of polyelectrolyte capsules loaded with Cascade Blue-labelled dextran was irradiated with an AMF (300 kHz, 24 kAm^{-1}) for 90 min and its fluorescence intensity was compared with capsules that were not irradiated as control. Fig. S-V.1 shows the results of the analysis of at least 400 different capsules of each sample (AMF treated and control). The fluorescence intensity was normalized. As it can be seen, the intensity of the capsules that were irradiated decreased compared to the control sample. This corresponds with the presence of Cascade Blue-labelled dextran released in the supernatant of the sample after AMF irradiation as detected by fluorescence spectroscopy. However, the capsules did not completely release the Cascade Blue-labelled dextran, most likely due to the polyelectrolyte matrix formed during the LbL assembly on porous CaCO_3 templates.² This partial release has been observed in similar capsules loaded with plasmonic nanoparticles and opened with infrared light.³

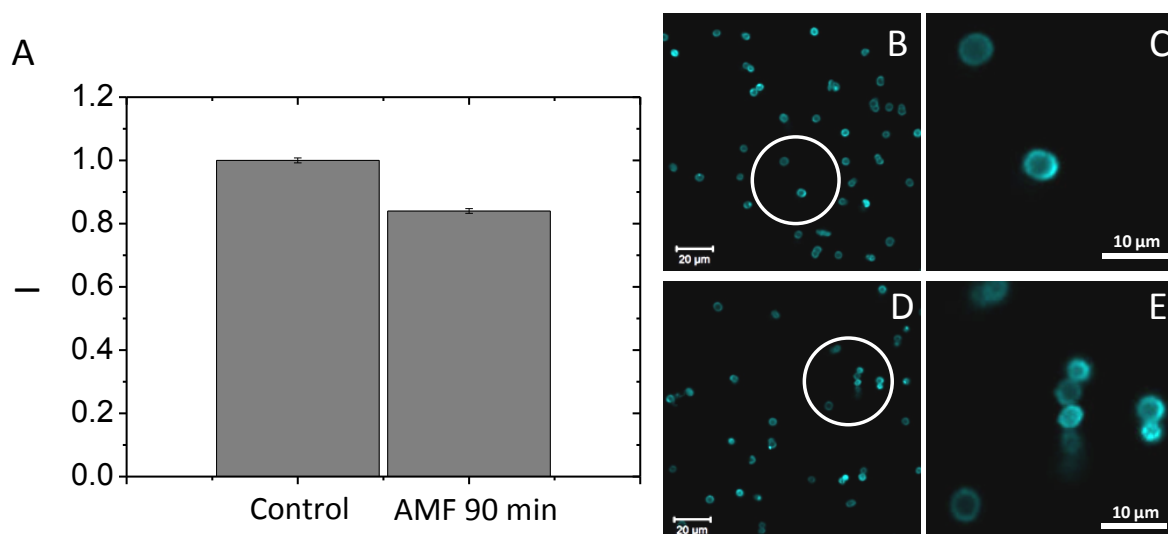


Fig. S-V.1 A) Normalized fluorescence intensity of polyelectrolyte capsules loaded with Cascade Blue-labelled dextran after RF irradiation for 90 min (24 kAm^{-1} , 300 kHz) compared with a control sample that was not irradiated. (B, C) Confocal images (blue channel) of the control sample. The white circle in B corresponds to the area shown in image C. (D, E) Confocal images (blue channel) of the polyelectrolyte capsules irradiated for 90 min. The white circle in D corresponds to the area shown in image E. The scale bar corresponds to 20 μm for (B, D) and 10 μm for (C, E).

VI) Hyperthermia experiments.

Hyperthermia experiments were carried out in a commercially available set up (DM100 Series, nanoScale Biomagnetics Corp.). To evaluate the specific absorption rate (SAR) of water soluble microcapsules (decorated with iron oxide nanocubes), a solution was introduced into a sample holder isolated from the system by a vacuum chamber in order to perform the measurements under close-to-adiabatic conditions. The SAR was measured at 300 kHz and 24 kAm^{-1} at three different iron concentrations: $1.6 \text{ g}_{\text{Fe}}/\text{L}$, $2.7 \text{ g}_{\text{Fe}}/\text{L}$ and $4.8 \text{ g}_{\text{Fe}}/\text{L}$. All reported SAR values were calculated according to the following equation:

$$\text{SAR} [\text{W} \cdot \text{g}^{-1}] = \frac{C}{c(\text{Fe})} \cdot \frac{dT}{dt}$$

Here $C = 4.187 \text{ kJ} \cdot \text{L}^{-1} \cdot \text{K}^{-1}$ is the specific heat capacity of water per unit volume and $c(\text{Fe})$ is the mass-concentration (in g/L of atomic Fe) of magnetic material in solution. The measurements were carried out in close-to-adiabatic conditions, thus the slope of the curve dT/dt was measured by taking into account only the first few seconds. It is worthy to underline that measurements done in pure water (blank experiment) did not show a temperature increase (see Fig. 2 of the main paper and Fig. S-VI.1). The calculated SAR values are summarized in Table S-VI.1. One may observe that the SAR decreases by decreasing the iron concentration. This trend is expected since a decrease in the iron concentration leads to a lower power generation. In this scenario, thermal losses due to a non-perfect adiabatic-condition become more relevant and the formula is not any more valid. In such conditions the calculated SAR values is underestimated.

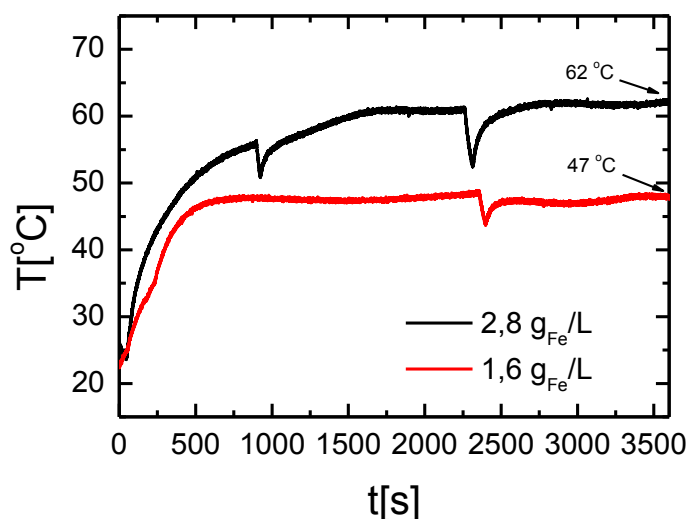


Fig. S-VI.1. Temperature as a function of time for $1.6 \text{ g}_{\text{Fe}}/\text{L}$ (red line) and $2.7 \text{ g}_{\text{Fe}}/\text{L}$ (black line) of a solution of polyelectrolyte capsules with integrated magnetic NPs placed under an AMF (300 kHz and 24 kAm^{-1}) for 60 minutes. The amount of iron was tuned by varying the amount of microcapsules. I.e. the amount of iron per capsule is the same, but the capsules concentration was varied in order to vary the amount of Fe in solution. During the experiment the solutions were removed from the cavity were the AMF was applied (dips in the curve at 900 s, 2350 s and 2450 s) in order to control and shake the solutions.

f [kHz]	H [kAm ⁻¹]	dT/dt [°C/s] = dT/dt [K/s]	c(Fe) [g/L]	SAR [W/g _{Fe}]
300	24	0.1	1.6	262
300	24	0.24	2.7	372
300	24	0.49	4.8	427

Table S-VI.1. SAR values measured at three different concentrations, 1.6 g_{Fe}/L, 2.7 g_{Fe}/L and 4.8 g_{Fe}/L at 300 kHz and 24 kAm⁻¹. Example for 4.8 g_{Fe}/L: SAR = C/c(Fe) · dT/dt = (4.187 kJ·L⁻¹·K⁻¹ / 4.8 g·L⁻¹)·0.49 K·s⁻¹ ≈ 427.4 W/g_{Fe}

For the AMF experiments at different concentrations, we observed that for low concentration of iron (below 4.8 g/L) the temperature achieved was below 80 °C. Absorption spectra for these samples were recorded (Fig. S-VI.2), showing a strong increase in the absorption at 270 nm, a feature also observed for the samples with an iron concentration of about 4.8 g/L. However, the signal-to-noise ratio was rather low together with a strong contribution of the absorption at low energy, which was attributed to the presence of polymer capsules with integrated magnetic NPs (Fig. S-VI.2). This observation lead to two main conclusions: First, samples need to be filtered in order to remove the contribution of free magnetic NPs, and second the amount of magnetic NPs in the capsules needs to be as high as much in order to get a better signal-to-noise ratio. In this regard a solution with an iron content of 4.8 g/L was used and treated for 90 minutes to ensure a better release of the Cascade Blue-labelled dextran. In addition, the supernatant was filtered by using Microcentrifuge Spin Cups and Columns (cut-off 100K). Notice that, as reported in the main manuscript, before the experiments, and after collecting the capsules with integrated magnetic NPs with a magnet and adding fresh Milli-Q water, the capsules with integrated magnetic NPs were again collected and the supernatant was analyzed in order to ensure that no free Cascade Blue-labelled dextran was present in the initial solution. It is worthy to underline that the increase in the absorption signal below 270 nm for low concentrated samples (2.7 g_{Fe}/L and 1.6 g_{Fe}/L) treated under an AMF suggests that, even at low temperature, microcapsules are damaged. The origin of this could be either a local increase of the temperature or through mechanical damaging of the shell during the AMF treatment. This point requires further investigation in future work.

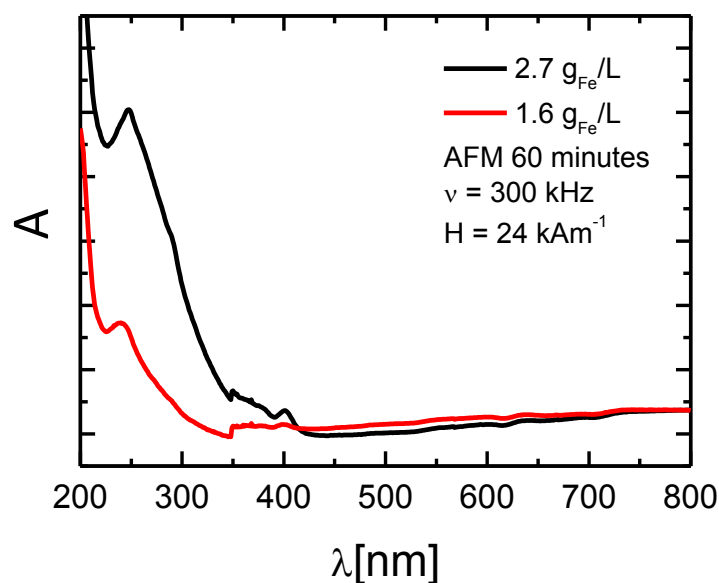


Fig. S-VI.2. UV-vis absorption spectra of the supernatant of two solutions of capsules with integrated magnetic NPs with iron content of 2.7 g/L (black line) and 1.6 g/L (red line) treated for 60 minutes under an AMF (300 kHz and 24 kAm⁻¹).

Note that heat mediated opening of capsules is an inhomogeneous process, i.e. heat due to the irradiated NPs is created a local spots of the capsule surface. Homogeneous exposure of the whole capsules to high temperatures (90 °C) in contrast tightens the capsule wall. This heat shrinking effect is actually used for improved encapsulation of cargo.⁴ We have performed a control experiment with nanoparticles in the capsule wall and encapsulated FITC-dextrane as cargo and no enhanced release upon heating to 90 °C was observed.

VII) References

1. P. Guardia, A. Riedinger, S. Nitti, G. Pugliese, S. Marras, A. Genovese, L. Manna and T. Pellegrino, 2014, DOI: 10.1039/C4TB00061G.
2. D. V. Volodkin, A. I. Petrov, M. Prevot and G. B. Sukhorukov, *Langmuir*, 2004, 20, 3398-3406.
3. M. Ochs, S. Carregal-Romero, J. Rejman, K. Braeckmans, S. C. De Smedt and W. J. Parak, *Angewandte Chemie International Edition*, 2013, 52, 695-699
4. K. Köhler, G. B. Sukhorukov, *Advanced Functional Materials* 2007, 17, 2053-2061.